Influence of damping and nonlinearity in plucked strings: why do light-gauge strings sound brighter?

J. Woodhouse*[1]

[1]Cambridge University Engineering Department, Trumpington Street, Cambridge CB2 1PZ, UK.

October 11, 2017

Abstract

When monofilament nylon strings of different tensions are used on a plucked instrument like the guitar or lute, it is readily observed that a lower-tension string tends to give a brighter sound. The elementary linear theory of a plucked string predicts no such effect. Linear theory can be extended to include bending stiffness and frequency-dependent damping: detailed measurements on a range of nylon strings are analysed to enable this extended model to be made quantitatively accurate. It is shown that a small influence of the string gauge is predicted, but synthesis based on this model does not match measurements or perceived differences of sound quality. Two nonlinear effects are then explored. The familiar effect of coupling between transverse and axial vibration in the string is shown to account for some observed features, but still does not explain the large difference of sound. The evidence from measurements strongly suggests that the mechanism responsible for the sound differences involves nonlinear interaction between the string and other parts of the structure, such as the frets. Because a lower-tension string tends to be played at larger amplitude, such "buzzing" interactions are more likely to occur. Implications for makers and players of instruments like the lute are discussed.

PACS numbers:43.75

1 Introduction

The guitar and the lute are both plucked-string instruments that commonly use plain monofilament nylon for their higher strings. The sound quality produced by the two instruments is significantly different. Several factors contribute to this difference, but it will be shown here that if well-understood factors are eliminated, a puzzle remains. These well-understood factors include the nature of the 'plectrum' used to excite the string (the classical guitar is usually played with fingernails, while the lute is usually played with the flesh of the fingertips), and the influence of the body resonances and sound radiation characteristics of the instrument. It will be suggested here that the remaining important factor is that lighter-gauge (and thus lower-tension) strings are used on the lute compared to the guitar.

Measurements will be shown in this paper of the transient vibration of four different gauges of nylon string, all fitted to the same guitar, tuned to the same fundamental frequency, and plucked in the same way. As will be explained in detail in section 3, this minimises many of the extra factors that can contribute to sound differences, but when played in a normal manner the four strings were clearly and distinctively different to the ear: the thinnest string sounded significantly brighter. The thinnest string was a Pyramid lute string of nominal gauge 0.525 mm, while the others were the top three from a set of d'Addario Pro Arte classical guitar strings, "Hard Tension". All the strings were marketed as "rectified" nylon, meaning that they have been centreless-ground to give a smooth surface finish and a well-controlled diameter.

*jw12@cam.ac.uk

Players are not surprised by the difference of sound between the strings: it is quite familiar. However, there does not appear to be any recognition in the scientific literature that the central phenomenon is at odds with the elementary account of the vibration of a plucked string, familiar from many books and undergraduate courses. Measurements on the four strings will be used here first to demonstrate that there really is a clear physical difference, and then to explore possible linear and nonlinear mechanisms that may contribute. The measurements are analysed to give detailed quantitative information about bending stiffness and frequency-dependent damping of the strings: an excellent match to standard models is obtained in both cases. The measurements also give clear evidence for nonlinear effects. Some of these observations can be explained in terms of the familiar geometric nonlinearity, leading to coupling between transverse and longitudinal string vibration: detailed analysis and predictions are shown for this mechanism. However, none of these effects turns out to account for the observed sound difference, and finally a tentative explanation will be advanced in terms of an entirely different nonlinear mechanism.

2 Measurements and preliminary analysis

It is a common experience in musical acoustics that an effect which seems obvious to the ear may prove surprisingly hard to pin down in physical measurements. It is therefore prudent to check whether the phenomenon of interest here has readily measurable consequences. For this purpose, some preliminary results for the four strings just described will be presented. The strings were all tuned using a standard electronic tuner to the nominal pitch E_4. It is not clear exactly how such tuners choose their compromise pitch for a stiff string, but empirically this tuning resulted in a fundamental frequency 327.5 Hz. A small accelerometer (DJB M222C) was fixed to the tie-block on the bridge of the guitar, on the bass side. This was used (through a suitable charge amplifier) to record the body vibration in response to plucks of the four strings, at a sampling rate of 80 kHz with 16-bit precision using a PC-based data-logger equipped with an acquisition card (National Instruments PCI-6250) and running software written in Matlab.

Plucks of two kinds were recorded. First, the strings were played in the manner of a lutenist, using the flesh of a thumb. Each pluck was done with the 'same' position and gesture, within the tolerance to be expected of a human performer. To obtain more controlled results, a second set of plucks was recorded using the wire-break method: a length of very fine copper wire is looped around the string, then pulled gently until it breaks. The result is a step function of force with a remarkably sharp front, with good repeatability of force amplitude and also with good control over the position and direction of the pluck. For the particular wire used here, the breaking force was 1.5 N. The plucks were applied at a distance of 30 mm from the bridge, in the direction normal to the soundboard of the guitar. In all cases the non-played strings were thoroughly damped to avoid any complications of sympathetic vibration.

The resulting time series data will be analysed in some detail in section 4, but the main phenomenon will be introduced here via a set of spectrogram plots, computed by taking the FFT of successive overlapping segments of the data. A Hanning window has been used on each segment to minimise artefacts. Frequency is plotted on the horizontal axis, up to the Nyquist frequency 40 kHz. Time is plotted upwards on the vertical axis, with the initial pluck at the bottom. The spectrogram amplitude in dB is indicated by the colour scale, auto-scaled relative to the largest value. As will be seen later, different aspects of the signals can be highlighted by choosing different lengths of FFT segment: this length controls the trade-off between time and frequency resolution [1]. For the plots in Figures 1 and 2, a length of 512 samples (6.4 ms) has been chosen.

The four spectrograms of Figure 1 should leave the reader in no doubt that audible differences will result. The two thicker strings show what would be expected: plucking with soft and rounded flesh results in vibrational energy being concentrated at low frequencies. The result for the thinnest string is strikingly different: a blaze of energy extends across the entire width of the plot. String 2 shows an intermediate result. The results from the wire plucks, shown in Figure 2, show less dramatic differences in line with expectations. The thicker strings now have energy across a much wider frequency range because of the localised and sharp pluck from the breaking wire. But there is still a clear trend towards more high-frequency energy in the thinner two strings. Probing the origins of these differences is the task of this paper. The first step is a careful examination of what differences can be attributed to linear theory.

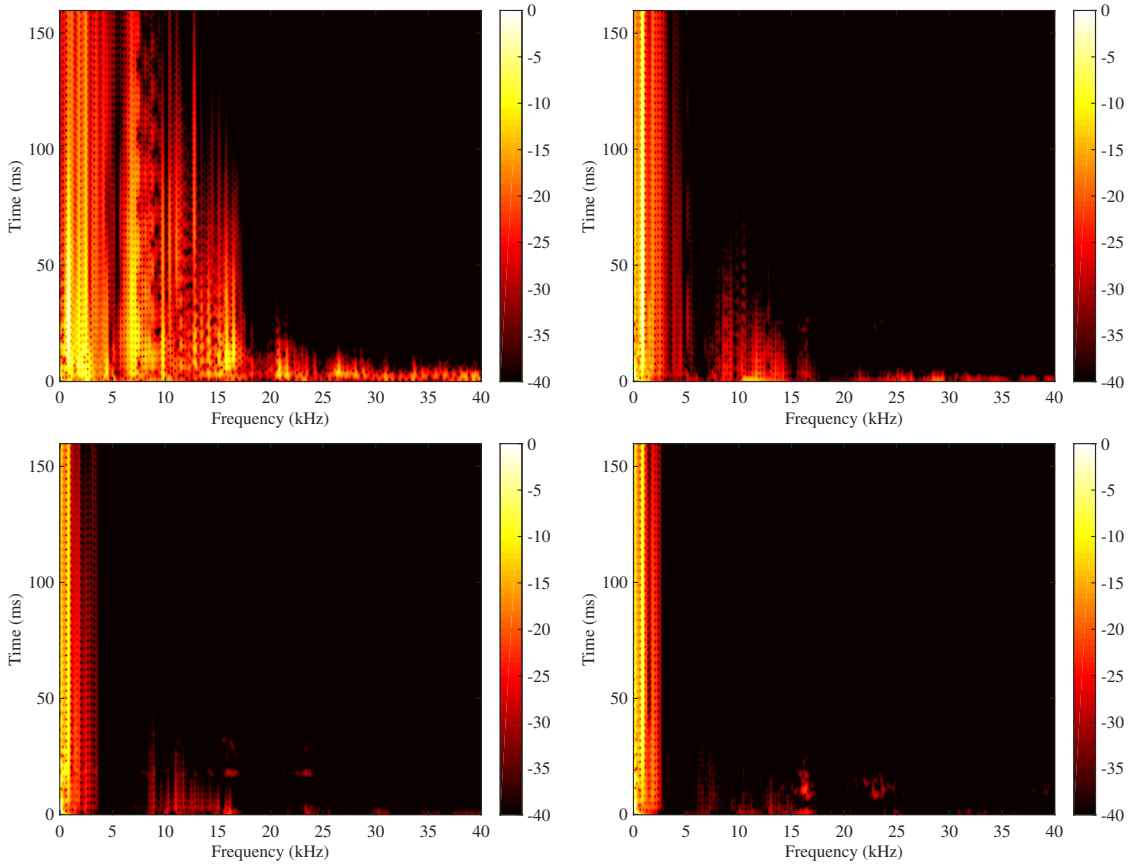

Figure 1: Spectrograms for the four strings following a conventional thumb pluck. Top row; string 1 (thinnest), string 2; bottom row; string 3, string 4 (thickest). (Colour online.)

3 Background theory

3.1 Frequency and impedance

The linear theory of vibration of a stretched string is very familiar, but some key results will be re-stated here because it is helpful to express them in a slightly unusual form. Consider a string of circular cross-section of radius a and length L, under tension T and made of material with Young's modulus E and density ρ. The nth natural frequency $\omega_n = 2\pi f_n$ satisfies

$$\omega_n^2 \approx \frac{T}{m}\left[\frac{n\pi}{L}\right]^2 + \frac{EI}{m}\left[\frac{n\pi}{L}\right]^4 \tag{1}$$

where $m = \pi a^2 \rho$ is the mass per unit length, and the second moment of area $I = \pi a^4/4$ (see for example Rayleigh [2]). This result follows from the Rayleigh quotient, and the approximation sign arises because it has been assumed that the corresponding mode shape is

$$u_n(x) = A \sin \frac{n\pi x}{L} \tag{2}$$

where $0 \leq x \leq L$ is the position variable along the length of the string and A is a normalisation constant to be discussed in section 3.3. A real string will deviate slightly from this assumption because of end effects: coupling to a non-rigid structure at both ends, and also possible effects of evanescent fields arising from the detailed end boundary conditions. Nevertheless, it will be seen in section 4 that equation (1) holds up very well for real strings.

The second term on the right-hand side of equation (1) arises from the non-zero bending stiffness of the string. For realistic musical strings, the bending stiffness effect is relatively weak so that the

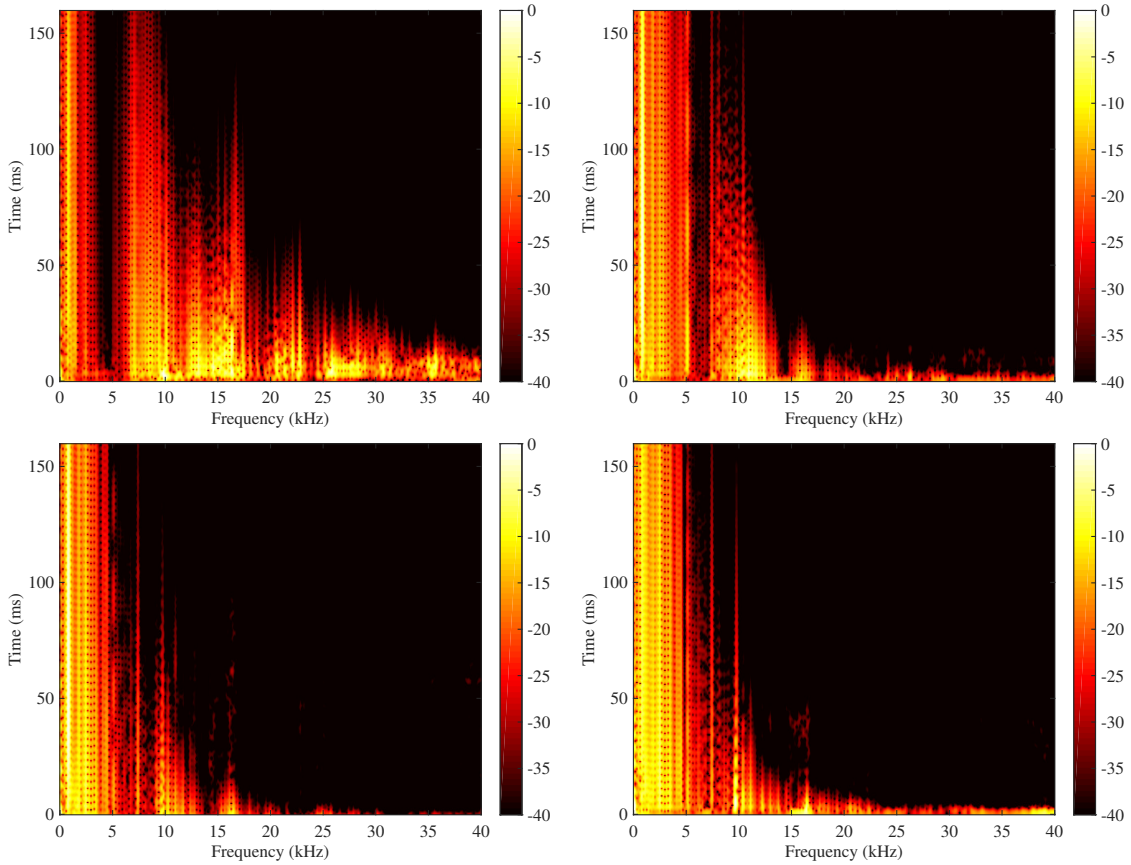

Figure 2: Spectrograms for the four strings following a wire-break pluck 30 mm from the bridge, from thinnest (top left) to thickest (bottom right). (Colour online.)

fundamental frequency (i.e. $n = 1$) is always well approximated by neglecting this term:

$$f_1^2 = \frac{\omega_1^2}{4\pi^2} \approx \frac{T}{m}\left[\frac{1}{2L}\right]^2. \tag{3}$$

For the experiment to be described here, all the strings have the same values of E, ρ, L and f_1. Equation (3) can thus be used to express the tension in terms of known quantities:

$$T \approx \left(\pi a^2\right) \times \left(4\rho L^2 f_1^2\right) \tag{4}$$

where the first bracketed term is the cross-sectional area, and the second one is thus the stress in the string. This demonstrates that a string of a given material and length, tuned to a given pitch, has a stress that is independent of the string radius a.

That fact is important for the results to be shown here. It has been shown [3, 4] that the mechanical properties of a nylon string depend significantly on the stress state and history. In particular, the Young's modulus can increase by approximately a factor 4 between the unstressed state before it is fitted to the instrument and the state just before it breaks. However, the four strings to be studied here all had the same stress state, and hence the same material properties. Furthermore, they had all been under tension long enough for creep processes to equilibrate: in musician's terms, the strings were well settled. This should eliminate any possibility of subtle influences, for example on internal damping, which may arise while creep is still active. As a result, any confounding factors associated with unknown, and probably non-linear, constitutive behaviour can be ignored provided interest is focussed on comparisons between the strings.

Physical properties of the four strings are summarised in Table 1. The first row shows the measured diameters of the four strings; all slightly lower than the nominal gauge according to the manufacturers,

since the strings are under tension. The diameters can be seen to cover roughly a factor of 2. The next row shows the corresponding calculated tensions: as shown in equation (4) the tension is proportional to the square of the string diameter, so that it varies by about a factor 4 here. However, as emphasised by the next row, the stress is identical in all four strings as just explained.

	String 1	String 2	String 3	String 4
String diameter $2a$ (mm)	0.50	0.69	0.78	0.96
Tension T (N)	39	75	95	144
Stress (MPa)	199	199	199	199
Mass/unit length m (g/m)	0.216	0.411	0.526	0.796
Impedance Z_0 (Ns/m)	0.092	0.175	0.224	0.339
Bending stiffness EI (N m^2)	0.037	0.134	0.218	0.500
n_{crit}	213	155	137	111

Table 1: Physical properties of the four tested strings, assuming values $\rho = 1100$ kg/m^3 and $E = 12$ GPa.

Substituting equation (4) into equation (1), the natural frequencies can be expressed in the form

$$f_n^2 \approx n^2 f_1^2 + \frac{E}{16\rho}\frac{n^4\pi^2 a^2}{L^4}. \tag{5}$$

For sufficiently high mode numbers n the bending term ceases to be a small perturbation. To give an indication of when this occurs, define n_{crit} as the value when the two terms in equation (5) have equal magnitude. The result is

$$n_{crit} \approx \frac{4L^2 f_1}{\pi a}\sqrt{\frac{\rho}{E}}. \tag{6}$$

Values for the four strings used here are listed in Table 1. Another important parameter for the string is the wave impedance

$$Z_0 = \sqrt{Tm} \approx 2\pi a^2 \rho L f_1, \tag{7}$$

values of which are also listed in Table 1.

The dependence on a revealed by equations (5–7) encapsulates two familiar but important trends: a thicker string will have higher inharmonicity due to bending stiffness, and it will have a higher wave impedance so that it will couple more strongly to the body of an instrument and so tend to produce louder sound for a given amplitude of string vibration.

3.2 Damping model

The next ingredient of linear vibration theory needed for this study concerns damping, and is somewhat less familiar. The damping factor of musical strings varies significantly with frequency [5, 6], and it is important for the present investigation to explore how it also varies with the string gauge. There are three main physical mechanisms of energy loss in a vibrating string: loss by coupling to the instrument body, viscous dissipation due to the surrounding air, and viscoelastic loss within the material of the string. All three effects can be estimated, and the resulting estimates will be compared to measurements in section 4.

Energy loss via the bridge to the instrument body will vary strongly with frequency, depending on the proximity of individual body resonances [7]. The details of body resonances are not of direct interest here, but a simple and useful approximation to the general level and trend of the energy loss can be obtained using the approach of Statistical Energy Analysis (see for example [8, 9]). In the sense of an ensemble average over many different instruments, or a frequency average of a single instrument, the guitar body will be felt by the string as a pure resistance, representing the point response of an infinitely-extended version of the soundboard (see e.g. [10, 8]). Denote this average resistance by Z_{body}. Published measurements (e.g. [7, 9]) show the bridge admittance of classical guitars tending to a roughly constant value at higher frequencies, and suggest a value for the effective resistance of the order of 300 Ns/m.

If for this purpose the string is approximated as an ideal flexible one (i.e. ignoring the bending stiffness perturbation), a wave impinging on this resistive termination will experience reflection with a

reflection coefficient

$$R = -\frac{1 - Z_0/Z_{body}}{1 + Z_0/Z_{body}} \approx -1 + 2\frac{Z_0}{Z_{body}} \tag{8}$$

and hence from equation (10) of Woodhouse [11], the loss factor of the nth mode of the string arising from this loss mechanism alone will be

$$\eta_{body} \approx \frac{2Z_0}{\pi n Z_{body}} \approx \frac{4\rho L f_1 a^2}{n Z_{body}} \tag{9}$$

using equation 7.

Energy loss due to viscosity in the surrounding air can be estimated using a classical analysis going back to Stokes. The associated loss factor is given by Fletcher and Rossing [12] in the form

$$\eta_{air} \approx \frac{\rho_a}{\rho}\frac{M^2}{2\sqrt{2}M + 1} \tag{10}$$

where ρ_a is the density of air, and

$$M = \frac{a}{2}\sqrt{\frac{2\pi f_n}{\eta_a}} \tag{11}$$

where η_a is the kinematic viscosity of air.

Energy loss from viscoelasticity in the nylon string is associated purely with the bending stiffness term: Young's modulus becomes a complex value $E(1+i\eta_E)$, and then an argument based on Rayleigh's principle [13] can be used to yield an expression for the associated loss factor of the nth string mode:

$$\eta_{bend} \approx \frac{E\eta_E I}{T}\left[\frac{n\pi}{L}\right]^2 \approx \frac{E\eta_E n^2\pi^2 a^2}{16\rho L^4 f_1^2} \tag{12}$$

after substitution of earlier results. The total modal damping factor can finally be estimated by

$$\eta_n \approx \eta_{body} + \eta_{air} + \eta_{bend}. \tag{13}$$

This estimate will be compared with measured results in section 4.

3.3 Pluck response

It will prove useful to be able to synthesise simplified predictions of the pluck response of a string, so the final piece of theory in this section relates to that. For the purposes of this paper, string vibration will be assumed to take place in a single plane, perpendicular to the soundboard of the instrument: all effects associated with the second polarisation of string motion, and its coupling to 3-dimensional body motion at the bridge, will be ignored. For an idealised pluck, a step function of force is applied to the string at a chosen position, with the string initially at rest. The force is non-zero initially, and falls to zero in the step as the 'plectrum' is released. In order to compare directly with the measurements, the required output variable is the acceleration induced in the instrument body. In the spirit of the approximations used in the previous subsection, the body is again represented by a simple resistance Z_{body}.

The transverse force exerted by the string at its termination can readily be calculated. For a step of magnitude P at position $x = \beta L$, this force is given by

$$f(t) = PT\sum_n \frac{u_n'(0)u_n(\beta L)}{\omega_n^2}\cos(\omega_n t)e^{-\omega_n\eta_n t/2} \tag{14}$$

where $u_n'(0)$ denotes the spatial derivative of the mode shape at the bridge, and the mode shapes must now be mass-normalised (see for example [14]), which requires

$$A = \sqrt{\frac{2}{\pi\rho L a^2}}. \tag{15}$$

This force evokes a velocity in the 'body' given simply by $f(t)/Z_{body}$, and then finally the acceleration $h(t)$ can be obtained by differentiation. After substitutions, and assuming small damping, the result is

$$h(t) \approx -\frac{8\pi f_1^2 P}{Z_{body}} \sum_n \frac{n \sin \pi\beta n}{\omega_n} \sin(\omega_n t) e^{-\omega_n \eta_n t/2}. \tag{16}$$

Note that there is no explicit dependence on a, except via the expressions for ω_n and η_n given above. If the effects of bending stiffness and frequency-dependent damping are not included, then linear theory predicts absolutely no influence of string gauge on the sound of a note plucked with a given force magnitude: this statement gives the essence of the puzzle mentioned in the Introduction. To explain the audible results and the measurements shown in Figures 1 and 2, either these additional details have a profound effect, or else something nonlinear must be involved.

For future reference, a closely related modal decomposition gives an expression for the initial shape of the string in equilibrium under the constant point force before the pluck: the transverse displacement is

$$u(x) = P \sum_n \frac{u_n(x) u_n(\beta L)}{\omega_n^2} = \frac{2P}{\rho \pi L a^2} \sum_n \frac{\sin \frac{n\pi x}{L} \sin \pi\beta n}{\omega_n^2}. \tag{17}$$

4 Calibration of linear model

4.1 Fitting the frequency and damping predictions

The next step is to analyse the results of the wire-break plucks of the four strings, to test how well the linear theory just described fits the observations and to explore the influence of string gauge within that linear theory. The wire-break plucks are chosen because they match most closely the assumptions of the theoretical calculations. The thumb plucks bring in additional unknown factors such as the precise shape and stiffness of the player's thumb, and effects associated with the second polarisation of string motion (which are minimised by the wire plucks). However, as has already been stated, the differences between the responses to wire plucks and thumb plucks pose less of a puzzle than the differences between the four strings in response to either kind of pluck.

The initial task is to verify the theoretical expressions derived in section 3, and obtain estimates of the parameters associated with bending stiffness and damping of the four strings. Modal frequencies and damping factors can be extracted from the pluck responses using methods described in some detail in previous papers [6, 9]. Each measured pluck signal can be used to compute a spectrogram, this time using longer FFT segments (4096 samples, 51 ms) to increase frequency resolution. A typical example is shown in Figure 3, for the wire pluck of string 2. To assist the reader in interpretation, the original time series is shown alongside the vertical axis, and the amplitude spectrum obtained by subjecting the entire time history to a long FFT is plotted (on a dB scale) alongside the horizontal axis. Each pluck response was recorded to a duration of 5 s to minimise issues of truncation, but the figure shows just the first 0.6 s for clarity.

As in Figures 1 and 2, the spectrogram amplitude in dB is indicated by the colour scale, auto-scaled relative to the largest value. The obvious parallel vertical lines of high amplitude show individual frequency components of the string's response, each decaying at its characteristic rate. Additional features just visible at early times and low frequencies come from vibration of the guitar body and background noise, but these do not interfere with the processing to be undertaken. Each frequency line can be detected, and the variation with time along that line analysed to give estimates of the frequency and damping factor: linear regression on the logarithmic amplitude gives the damping, while linear regression on the evolving phase allows the frequency to be calculated to much greater accuracy than would be given by the relatively coarse FFT bin spacing used to calculate the spectrogram.

The analysis just described can be carried out automatically, but the final stage needs some human intervention. In order to compare the results with the linear predictions from section 3, it is necessary to associate each frequency line with a particular mode number n. As has been described in some detail previously, the pattern of frequency peaks in a plucked guitar note like this is a little unexpected. At low frequency the anticipated series of approximately equally-spaced frequencies is seen, but at higher frequencies additional peaks appear: they can be seen in Figure 3 in the frequency range around 10 kHz, producing additional vertical lines in the spectrogram. Figure 25 of Woodhouse [6] shows a zoomed-in

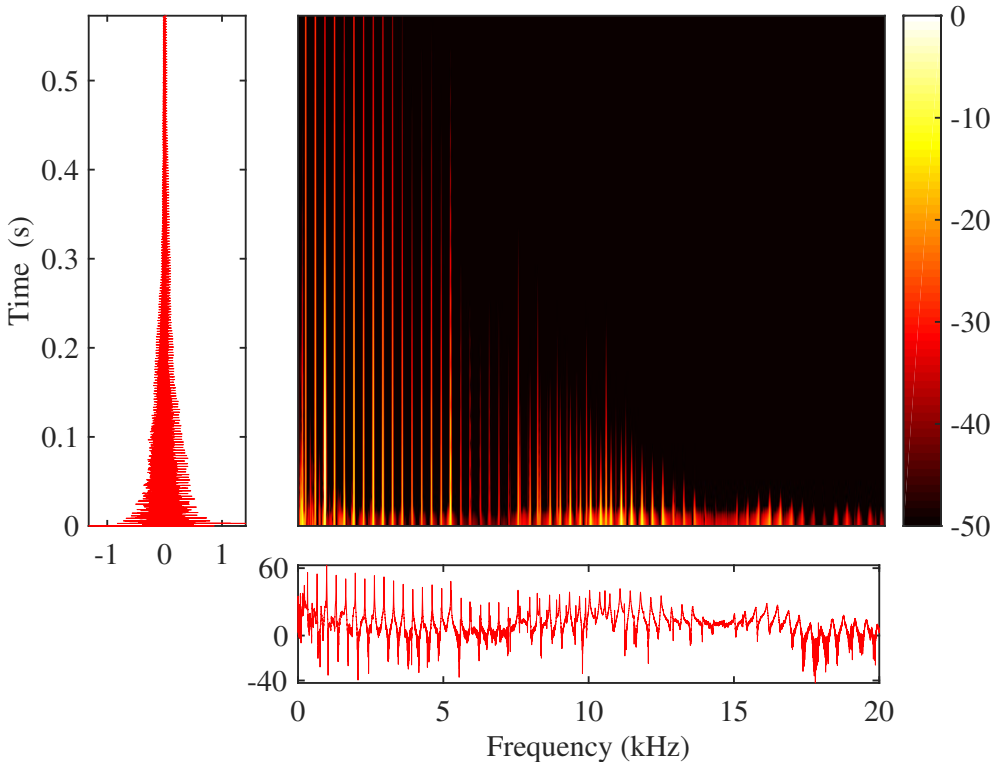

Figure 3: Example spectrogram showing the wire pluck of string 2. (Colour online.)

view of a typical cluster of peaks. Those earlier measurements typically showed four peaks, because both polarisations of string motion were included. However, the present measurements have been designed to minimise the influence of the second polarisation, and they typically show pairs of peaks. Close examination of the present results (not visible at the plotting scale of Figure 3) confirms that these pairs are indeed not associated with the two polarisations of transverse string motion. For reasons that will soon become clear, it is convenient to allocate the same 'mode number' n to the multiple peaks in each group. That allocation process was carried out by hand, based on the pattern of peaks in the frequency domain.

The results of this analysis are first used to test the predictions of equation (5) for the mode frequencies. The most useful thing to plot is not f_n directly but the reduced quantity f_n/n: for an ideal string with harmonic natural frequencies this quantity would be independent of n, but from equation (5) it is in fact expected to increase with n because of the influence of bending stiffness. Figure 4 shows the results, for the four strings. The discrete plotted points show the measurements, while the solid curves show the predictions of equation (5) using the measured string diameters shown in Table 1. For this purpose, values ρ =1100 kg/m^3 and E=12 Gpa were used: the former is typical of values listed in reference sources, while the latter is considerably higher than typical values for bulk nylon, but is consistent with the measurements of Lynch-Aird [4] on nylon strings at playing tension. It should be noted that Young's modulus for a viscoelastic material like nylon is frequency-dependent: the value chosen here is representative of measurements at frequencies in the kHz range.

It is clear that the measured frequencies fall into two groups for each string, corresponding to the split peaks mentioned above. One group (plotted as stars) matches the theoretical prediction very well, while the other group (plotted as circles) lies nowhere near it. However, this second group matches a frequency-doubled version of the theoretical prediction, shown by the dashed lines in the plots: it can be concluded that there is a nonlinearity operating in the plucked string, of a predominantly quadratic nature. Similar frequency-doubled peaks have previously been identified in measurements on pianos, in which context they are sometimes described as "phantom partials" (see for example [15]). Most likely, this nonlinearity is associated with coupling to axial deformation of the string. The simplest manifestation is the effect of variation in mean tension arising from length changes in the string during the transverse vibration, as

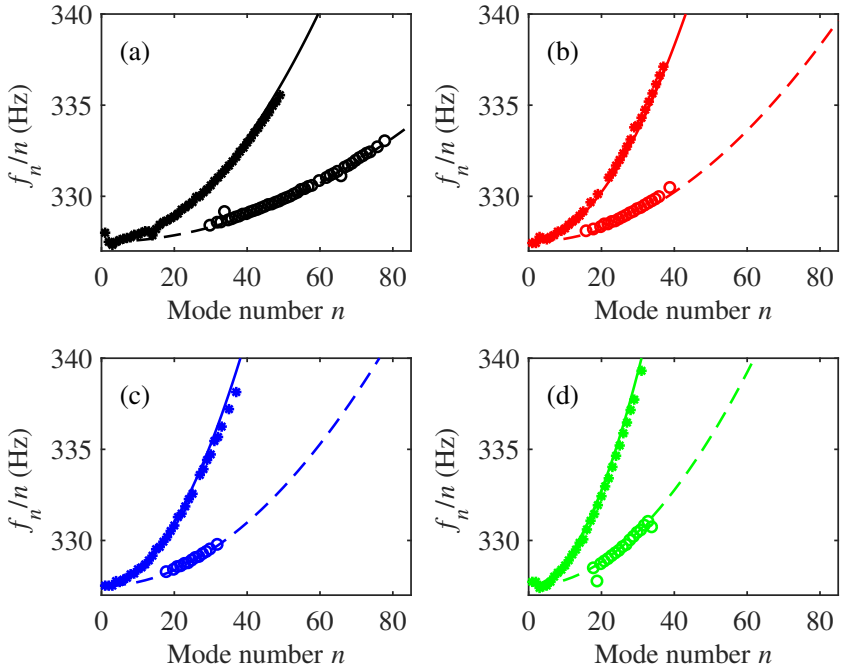

Figure 4: Reduced frequency f_n/n plotted against mode number n for (a) string 1; (b) string 2; (c) string 3 and (d) string 4. Discrete symbols show measured values. Solid lines show the fits to equation (5), using the measured string diameters and values $\rho = 1100$ kg/m^3 and $E = 12$ Gpa. Dashed lines show frequency-doubled values: see text. The colour coding of plots relating to the four strings will be used consistently in all figures. (Colour online.)

has been extensively studied in the past (for example [16, 17]). For any single string mode, it is obvious that the modulation of length, and therefore of tension, occurs at twice the frequency of the vibration. However, as will be explored in more detail in section 5.1, the wide frequency range involved in these tests requires a more careful analysis, involving coupling to the axial resonant modes of the string.

Returning to the question of validating and calibrating the best linear model, Figure 5 shows the results for damping factors of the four tested strings. The discrete symbols show the measured points, while the various lines indicate the theoretical comparison. Star and circle symbols are used to match those in Figure 4. The three separate contributions η_{body}, η_{air} and η_{bend} all appear as straight lines in this log-log plot. The predictions of η_{body} and η_{air} require almost no additional parameters, apart from textbook values for the density (1.2 kg/m^3) and kinematic viscosity (1.5×10^{-5} m^2/s) of air. To calculate η_{bend} a loss factor $\eta_E = 0.025$ was used, which is comparable with earlier published results [6]. Only one "fudge factor" was employed: a better fit to the data was obtained by reducing the estimated air damping by a factor 0.7, which is within the range of accuracy to be expected from the rather crude approximation used to obtain the formula.

The sum of the three contributions is shown as a solid curve for each string, and it is immediately clear that this curve follows the trend of the "star" data points remarkably well for all four strings. In each case, the points plotted as circles correspond to the points identified in Figure 4 as being associated with the quadratic nonlinearity. These points are somewhat scattered, but appear more or less where they would be expected: if a decaying sine wave is squared, the frequency is doubled and the decay rate is also doubled, so the effective loss factor remains unchanged. As a result, the points should appear horizontally shifted in Figure 5, by an amount representing a factor of 2 in frequency.

Some interesting details emerge from these plots. The lines representing η_{body} and η_{air} show somewhat similar trends, but the one for η_{air} is always higher: within this approximation of representing the body as a simple resistance, air damping is always stronger than body damping. The balance of the two, however, depends on the string gauge. For the thinnest string (string 1) the body damping is lower by an order of magnitude, whereas for the thickest string (string 4) the two are comparable, especially at lower frequencies. Notice that for the thinner strings the disparity is so great that the solid curve follows

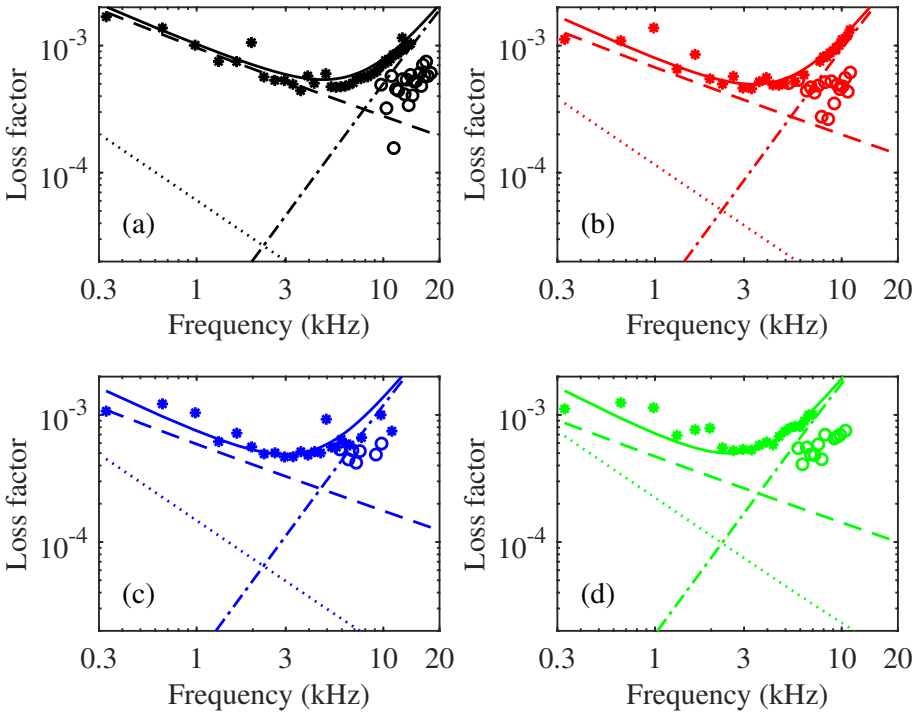

Figure 5: Loss factor η_n plotted against frequency for (a) string 1; (b) string 2; (c) string 3 and (d) string 4. Discrete symbols show measured values: symbols * and o match those used in Figure 4. Solid lines show the fit to equation (13), while the three straight lines show the separate contributions of equations (9) (body, dotted), (10) (air, dashed) and (12) (bending stiffness, dash-dot). (Colour online.)

the dashed curve for η_{air} at the lowest frequencies, but for string 4 the combined curve is significantly different: it matches the data points more closely than the dashed line, so this case gives a direct test of the influence of η_{body}.

The measured points show significant scatter around the predicted curves at low frequencies, and this would be expected. At low frequencies the variation of string-body coupling strength resulting from individual body resonances is much stronger than it is at higher frequencies, as has been explored in detail in earlier work [7]. The observed scatter in damping values is thus likely to be the result of small-scale variations in η_{body} with frequency, depending on the proximity of body resonances. It would be easy in principle to incorporate these effects in the predictions, as has been done in earlier work on guitar synthesis [6, 7]. However, for the present purpose the effects of the body become rapidly less important at higher frequencies and it can be argued that for the purposes of fitting the behaviour over a very wide frequency range the simple approximation captures the essence of the behaviour with a minimum of distracting details.

4.2 Comparisons with linear synthesis

Ignoring the nonlinear effects for the moment, the level of agreement with theory shown by Figures 4 and 5 is impressive. To reiterate, both plots were calculated using a single set of material parameters, and the differences between the strings come entirely as a result of using the measured values of a in the theoretical expressions. It appears that this set of parameter values captures any differences arising from linear effects rather accurately, and differences can indeed be seen in both plots. As expected, the effect of bending stiffness is more pronounced for thicker strings. Less obviously, there is a subtle but clear difference between the strings in the pattern of frequency-dependent damping.

An important detail of the linear model is highlighted in Figure 6. This shows the computed initial static deformation of the strings before the release of the pluck, from equation (17). The differences in tension lead to differences in absolute amplitude, but even the thinnest string is only displaced about 1 mm by the plucking wire. The inset plot shows the detailed behaviour near the plucking point. The

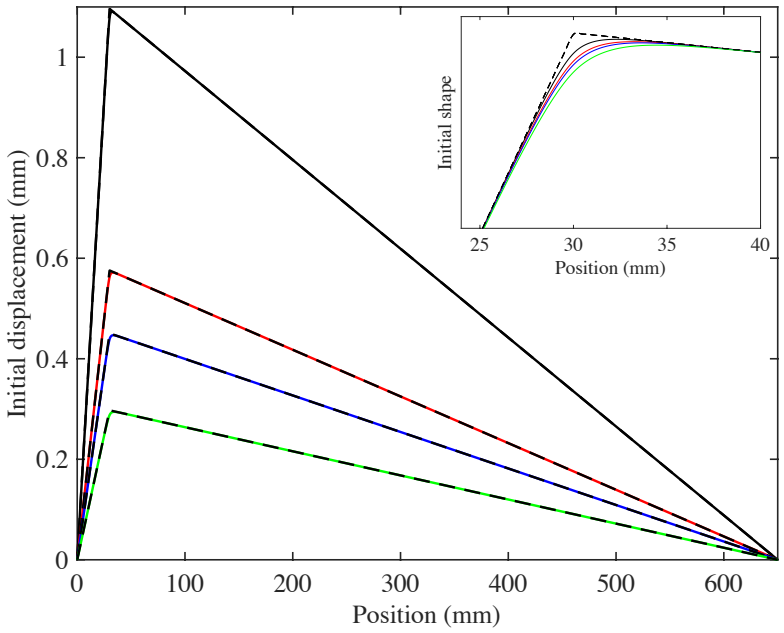

Figure 6: Initial pluck shapes for the four strings. Main plot: absolute displacements in response to the 1.5 N applied force; Inset: zoom view near the plucking point, with the curves normalised to identical nominal displacements, to show the influence of bending stiffness. The dashed lines indicate the response of corresponding ideal flexible strings. (Colour online.)

shapes have been normalised to the same nominal displacement in the absence of bending stiffness, and the colours indicate the actual predicted shapes of the four strings. It can be seen that the higher the bending stiffness, the more rounded the initial corner, exactly as would be expected.

Are these various linear effects sufficient to solve the original puzzle? The linear model can be used to synthesise ideal pluck responses of the four strings, using equation (16). A set of spectrograms based on the synthesised responses is shown in Figure 7, in a format directly comparable with Figure 2. It is immediately clear that the appearance of the two sets of plots is very different. Agreement could only be claimed in very broad terms: for example, the frequency-dependent damping has been captured quite well in the model, so it is not surprising that the general pattern of decay rates is mirrored in the synthesised results.

Most tellingly, the sounds resulting from the linear synthesis can be assessed directly. Only informal listening tests have been done, but the very clear impression is that the four strings give predictions that sound almost identical. There are very subtle differences, enough that a careful listener could probably tell them apart, but nowhere near as strong as the differences between the measured pluck sounds, either with thumb or wire.

5 Nonlinear effects

5.1 Coupling to axial string motion

The conclusion is that something nonlinear must be occurring, sufficiently strongly to produce the differences just described. The obvious first candidate is the quadratic nonlinearity already noted. It is fairly straightforward to make a preliminary investigation of this effect: the transverse string motion already simulated from the linear model can be used to calculate at leading order the induced axial string motion. (A related approach has been applied to piano strings by Bank and Sujbert [18].) The equations governing the coupled transverse-axial vibration of a string have been given by Morse and Ingard [19] (see equation 14.3.7). If the transverse string displacement is written $u(x,t)$ and the corresponding

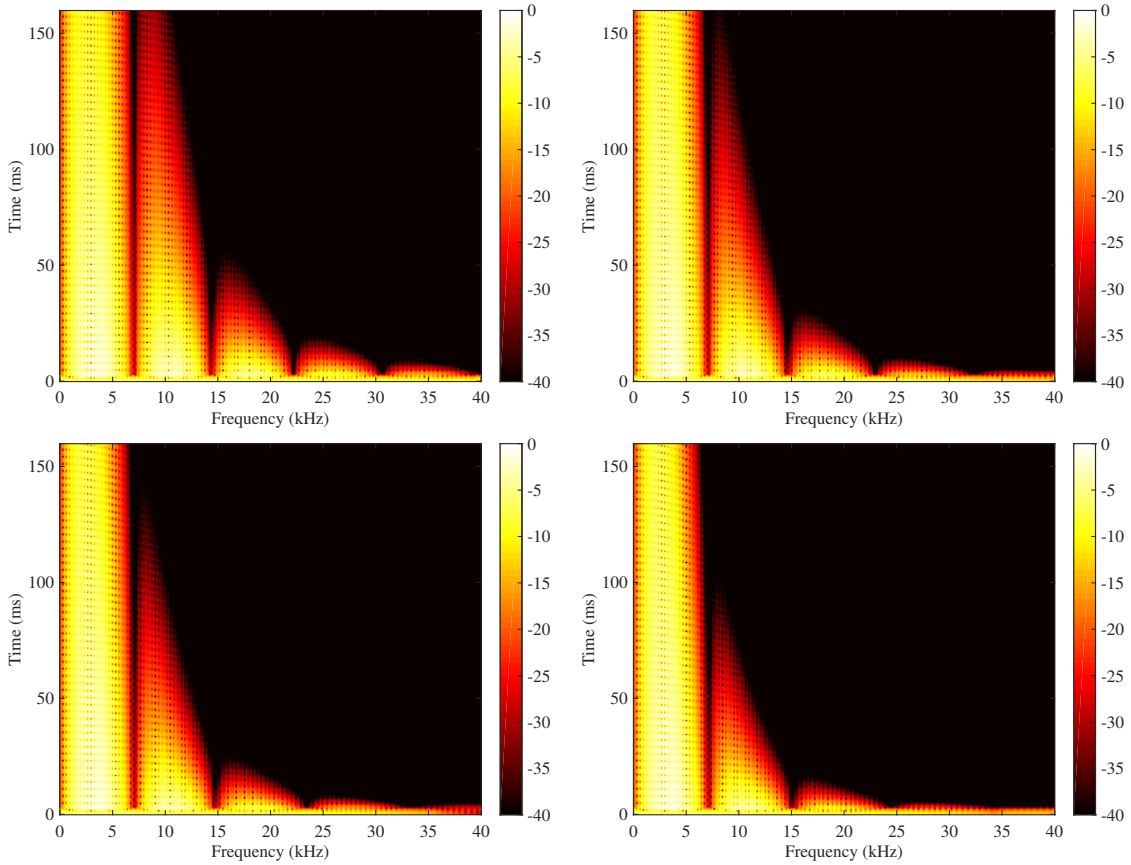

Figure 7: Spectrograms of the synthesised motion of the four strings, in the same format as Figures 1 and 2. (Colour online.)

longitudinal displacement $v(x,t)$, then

$$\frac{\partial^2 v}{\partial t^2} - c_l^2 \frac{\partial^2 v}{\partial x^2} \approx \frac{c_l^2 - c_t^2}{2} \frac{\partial}{\partial x} \left[\frac{\partial u}{\partial x} \right]^2 \tag{18}$$

where $c_t = \sqrt{T/m}$ is the transverse wave speed and $c_l = \sqrt{E/\rho}$ is the longitudinal wave speed.

It is not entirely clear what the boundary conditions should be for the longitudinal string motion, but if it is assumed that the end points of the string are fixed then the nth axial mode will take the simple form

$$v_n(x) = \sin \frac{n\pi x}{L} \tag{19}$$

with corresponding natural frequency $\omega_n^{(a)} = nc_l\pi/L$. Using the parameter values specified earlier, $c_l = 3230$ m/s, and the predicted fundamental frequency for all four strings on the guitar is about 2.5 kHz. This was directly confirmed by "squeaking" the strings into axial motion using fingers coated with violin rosin, and finding the frequency spectrum of the resulting (loud) noise.

Approximate solutions to equation (18) can computed by expressing the axial motion as a modal superposition

$$v(x,t) = \sum_{n=1}^{N} a_n(t) v_n(x) \tag{20}$$

where a suitable truncation value N can be chosen by ensuring that all modes within the audible frequency range are included: the value $N = 12$ has been used here. Define

$$p(x,t) = \left[\frac{\partial u}{\partial x} \right]^2, \tag{21}$$

the squared slope of the (known) transverse motion $u(x,t)$. The modal amplitude $a_n(t)$ can then be found by convolution of the modal generalised force with the relevant impulse response:

$$a_n(t) = \int_0^t g_n(t-\tau) q_n(\tau) d\tau \tag{22}$$

where

$$g_n(t) = \frac{1}{\omega_n^{(a)}} \sin(\omega_n^{(a)} t) e^{-\omega_n^{(a)} \eta_E t/2} \tag{23}$$

and

$$q_n(t) = \frac{c_l^2 - c_t^2}{L} \int_0^L \frac{\partial p}{\partial x} \sin \frac{n\pi x}{L} dx = -\frac{n\pi (c_l^2 - c_t^2)}{L^2} \int_0^L p \cos \frac{n\pi x}{L} dx \tag{24}$$

using integration by parts. To reiterate, $p(t)$ is calculated from the linear synthesis developed in section 4 and is taken as a known input function in the present nonlinear analysis.

A convenient output variable to compute is the axial force exerted at the bridge,

$$F^{(a)}(t) = \pi a^2 E \left. \frac{\partial v}{\partial x} \right|_{x=0} + \left[\frac{\pi a^2 E}{2} - \frac{T}{2} \right] \left. \left[\frac{\partial u}{\partial x} \right]^2 \right|_{x=0} . \tag{25}$$

This can be compared with the lateral force exerted on the bridge by the transverse motion, computed using the linear model presented earlier. The first term on the right-hand side contains the direct effect of the axial string motion, and can be evaluated as

$$\frac{\pi^2 a^2 E}{L} \sum n a_n(t). \tag{26}$$

The second term of equation (25) contains two elements, both involving the squared slope of the transverse displacement: one arises from the derivation of equation (18) (see equation (5) of Bank and Sujbert [18]), the other represents the resolved component in the horizontal direction of the tension at the bridge.

The early parts of these two waveforms, for all four strings, are shown in Figure 8, with the axial force displaced vertically by 1 N for clarity. The four strings are indicated by the same colour coding as in previous figures. The four lateral force waveforms are quite similar, while the axial force waveforms have a similar shape but different amplitudes for the four strings: the thinnest string gives the largest force.

In order to combine these two synthesised force waveforms to allow comparison with the measurements, it is necessary to know something about the vibration response of the guitar body to forces in the two directions. Figure 9 shows the results of direct measurements on the test guitar, in which force was applied using a miniature impulse hammer (PCB 086D80) on the bridge saddle at a position in the middle of the four tested strings, and response was measured using the same accelerometer as in the pluck tests shown earlier. Force was applied in the direction normal to the soundboard to give the response to transverse string vibration in that polarisation, and also parallel to the strings to give the response to axial forces in the strings.

The two transfer functions show different trends with frequency: the accelerance for the vertical force is higher at low frequencies, but the accelerance for axial force rises more rapidly with frequency, on average, and the two curves cross in the vicinity of 5 kHz. In the frequency range where the nonlinear effect was most apparent in the measurements shown in section 4.1, the two transfer functions have broadly similar magnitudes. Since Figure 8 showed that the forces are also of similar magnitude, it is not surprising that the nonlinear effect showed up so clearly in the measurements.

The steeper trend with frequency of the axial accelerance is easy to explain. The guitar soundboard is receiving a moment input rather than a normal force input from the axial string force, so the formula for response expressed as a modal superposition will involve the spatial derivative of the mode shapes in the direction parallel to the strings. This will produce a factor of the wavenumber component in that direction, and for bending waves in a plate the wavenumber is proportional to the square root of the frequency.

With the two measured transfer functions, it is straightforward to combine the two synthesised force signals. The force waveforms shown in Figure 8 are converted to the frequency domain by FFT, each is

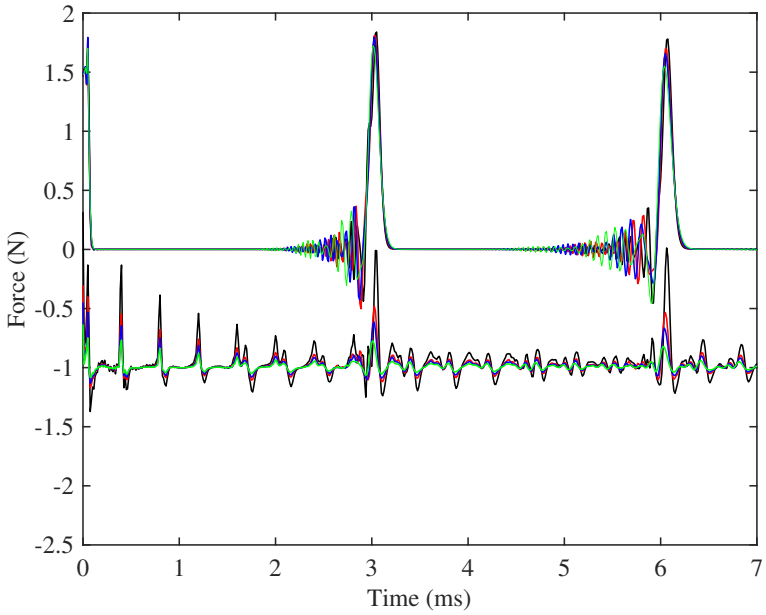

Figure 8: Comparison of force waveforms for the four strings. Upper curve: linear synthesis of transverse force at bridge; lower curve: non-linear synthesis of axial force at bridge (offset for clarity). (Colour online.)

multiplied by the relevant transfer function, the results are added, then an inverse FFT gives a combined transient time history. That time history can then be analysed as before. Figure 10 shows a comparison of spectrograms for the two extreme strings: string 4 (thickest) and string 1 (thinnest). For convenience of comparison, the relevant results from Figures 2 and 7 are included, and the results of the new combined synthesis shown below them.

For string 4, the comparison is quite encouraging. Although the new synthesis is by no means identical to the measurement, some key features are successfully reproduced. The texture of the spectrogram has become more "speckly". More strikingly, vertical lines around 7.5 and 10 kHz appear clearly in both measurement and simulation, but they were absent from the linear simulation. These are resonance frequencies for axial string motion. Fitting the decay rates in both cases shows that these features have an effective Q factor of the order of 10^3, like the transverse string modes, whereas the axial modes on their own, with the assumed loss factor of 0.025, would have a Q factor of only 40. What is being seen is resonant enhancement of the driven axial motion near the axial resonances, as discussed in slightly different terms by Bank and Sujbert [18]. Note that the simple theoretical approach being used here makes no allowance for any reverse influence of the axial motion on the transverse motion (such as additional energy loss). Given this slight uncertainty, the level of agreement between measurement and simulation is very satisfying.

For string 1, however, the comparison is less convincing. Although the speckly texture is still evident, and traces of the vertical lines can be seen, the overall pattern of the spectrogram of the measurement looks quite different from either simulation. Furthermore, informal listening tests using sound files generated from the measured and synthesised transient waveforms reveal very clearly that something is still missing from the modelling. The measured waveforms sound strikingly different, especially for string 1. In fact, the sounds of these accelerometer measurements are much more obviously different than the original acoustical sounds from the guitar, presumably because the accelerometer emphasises the higher frequencies where differences are bigger. The synthesised waveforms, on the other hand, are very similar-sounding. It is possible to tell that they are different, perhaps more different than the results of linear synthesis, but the differences are still quite subtle. Interestingly, in the context of piano acoustics it has been claimed that these "phantom partials" are important for realistic sound quality (see for example [20, 18]). Exploring this question across the wide range of stringed musical instruments may be a profitable subject for future research.

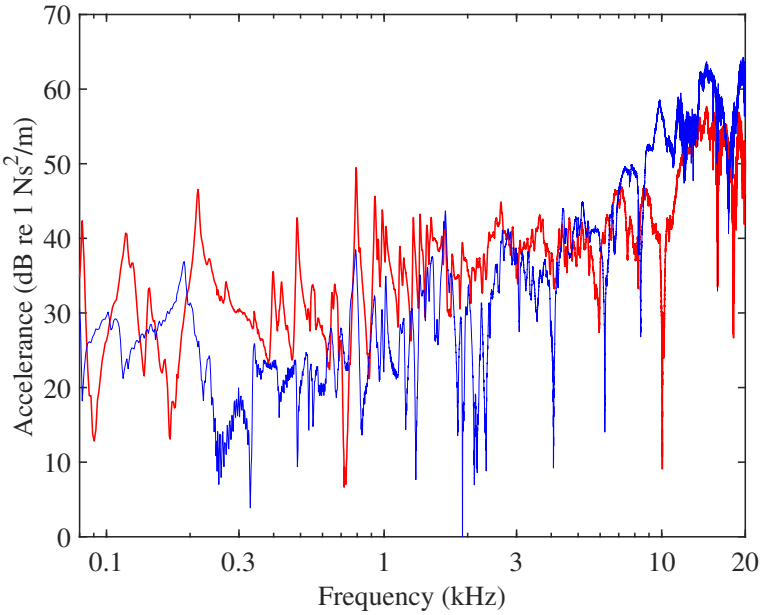

Figure 9: Measured accelerances for the guitar used in the experiments: accelerometer response to a vertical force (red curve) and an axial force (blue curve) on the bridge saddle, centrally positioned among the four tested strings. (Colour online.)

5.2 Nonlinearity from impacts

The conclusion for the present investigation is that another nonlinear mechanism must be operating. Clues can be gained by further analysis of the measurements. All four synthesised results in Figure 10 share a common feature: there is a minimum of response around 8 kHz, and at multiples of that frequency. This is a consequence of the chosen plucking position, 30 mm from the bridge with a total string length of 650 mm. String modes with numbers close to $650/30 \approx 22$ have a nodal point near the plucking position, so that little energy is input at the corresponding frequency. The measurement for string 4 shows a trough at a similar frequency, but the measurement for string 1 shows a trough at a much lower frequency around 4 kHz.

An alternative view of this effect is given by Figures 11 and 12, which show the corresponding comparisons of high-resolution spectra for the same six cases as Figure 10. For string 4, the measurement shows a recognisably similar pattern to the combined linear/nonlinear synthesis, with a minimum of peak heights occurring a little below 8 kHz and further minima around multiples of that frequency. Careful inspection shows a pattern of additional peaks, with at least a qualitative correspondence to those attributed to the nonlinearity in the discussion of section 4.1. Further analysis, not reproduced here, confirms that the nonlinear signal computed from equation (25) reproduces the frequency-doubled pattern marked by the dashed lines in Figure 4.

Figure 12 tells a different story for string 1, though. This time the measurement shows large peaks around the frequency where the trough is predicted. This strongly suggests that there must be a source of vibration excitation at a different position on the string than the plucking point. To look for direct evidence of this it is useful to examine spectrograms calculated using very short individual FFTs, to resolve temporal features in the very early part of the transient vibration. Figure 13 shows a set of plots in the same layout as Figure 10, using an FFT length of 64 samples (0.8 ms). Note that similar early-time spectrograms for plucked strings have been shown and discussed in an earlier paper [6].

The results of linear synthesis for both strings show a similar pattern. Very soon after the initial pluck, the first disturbance reaches the bridge and produces a bright stripe across the bottom of each plot. Nothing is then seen until the first reflection arrives back at the bridge from the other end of the string, producing a ridge that is curved because of the wave dispersion resulting from bending stiffness. After that a pattern of multiple reflections follows. The heights of the ridges can be seen to be modulated in frequency by the pattern just discussed, with minima just below 8 kHz and at multiples of that frequency.

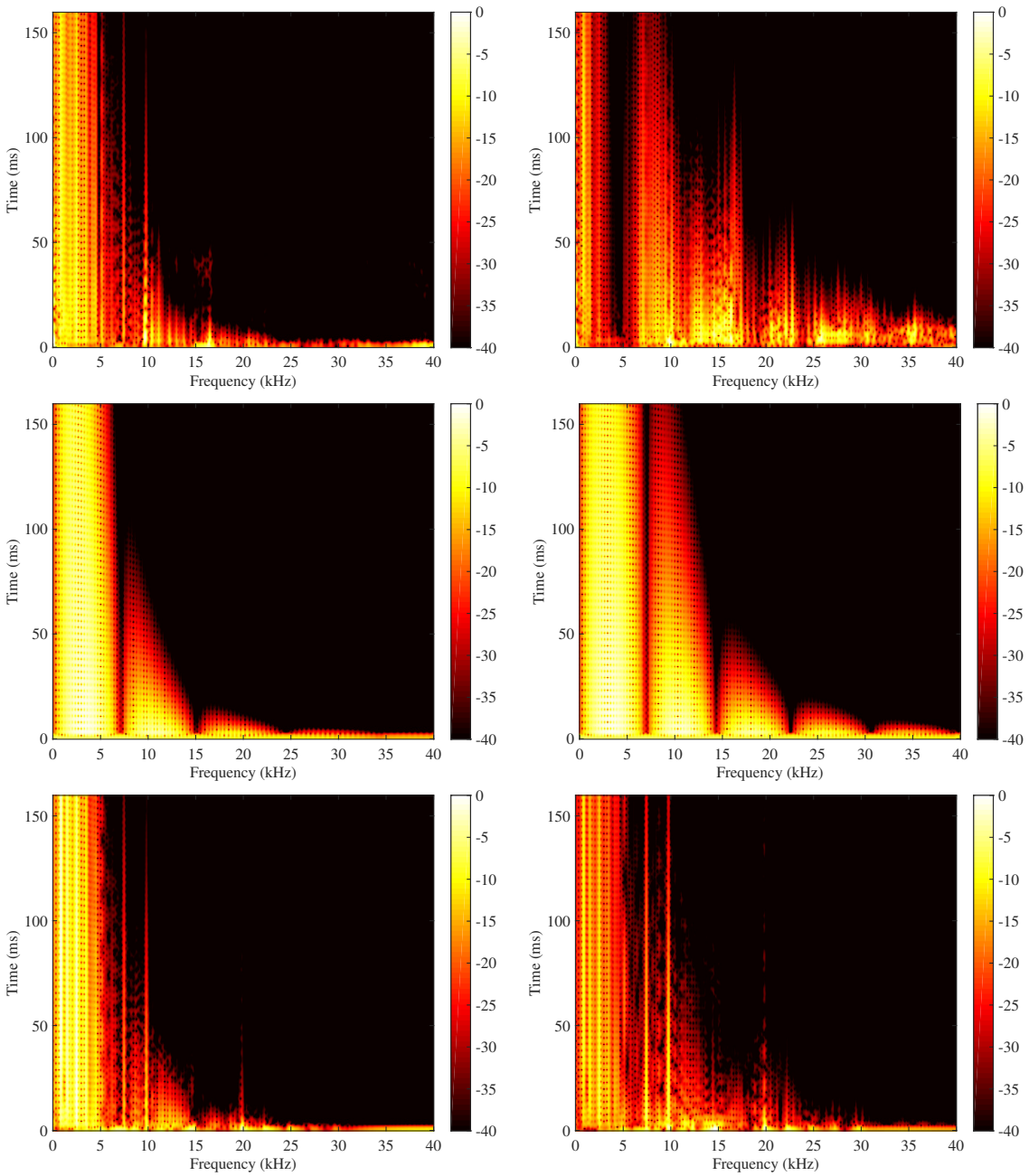

Figure 10: Spectrograms for string 4 (left column) and string 1 (right column), calculated with the same settings as Figures 1 and 2. Top row: wire-pluck measurements; middle row: linear synthesis; bottom row: combined linear/nonlinear synthesis. (Colour online.)

For the combined linear/nonlinear synthesis a similar pattern can be seen, but some of the empty space has been filled in because additional disturbances can now travel on the string at the (much faster) axial wave speed.

For string 4, the measurement shows a pattern that is at least qualitatively similar: the curving ridges can be discerned, the modulation in frequency is visible, and there is a texture of infill between the ridges. The measurement for string 1 shows something quite different. Note that the plotted spectrograms are all auto-scaled from the highest value. The top right-hand plot in Figure 13 shows very little trace of a bright stripe along the bottom of the plot, because the auto-scaling has been based on some far higher signals occurring one or two periods after the pluck. For example, notice the bright patches around 15

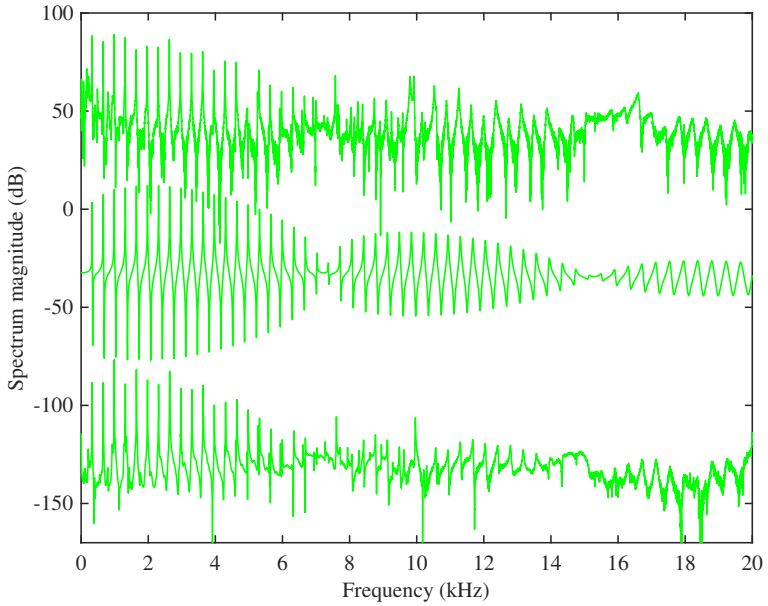

Figure 11: Comparison of spectra for string 4. Upper curve: wire-pluck measurements; middle curve: linear synthesis; bottom curve: combined linear/nonlinear synthesis (offset for clarity). (Colour online.)

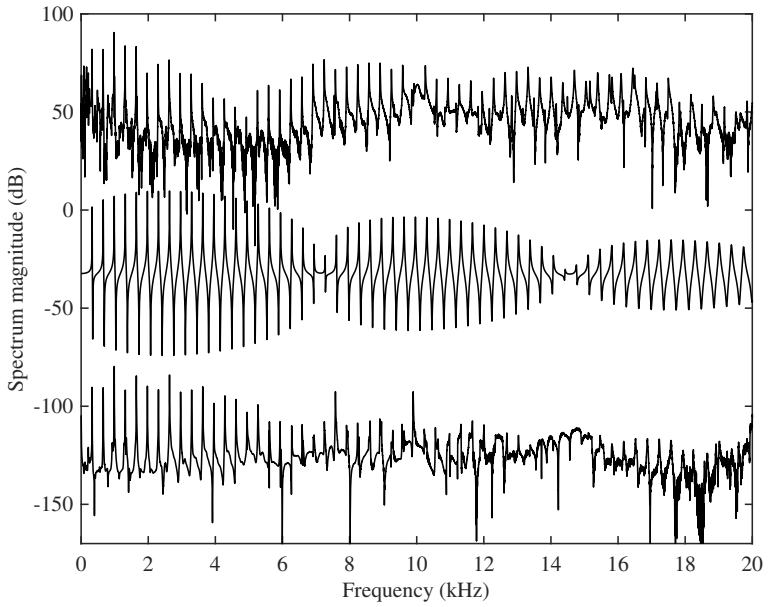

Figure 12: Comparison of spectra for string 1, in the same format as Figure 11. Upper curve: wire-pluck measurements; middle curve: linear synthesis; bottom curve: combined linear/nonlinear synthesis (offset for clarity). (Colour online.)

and 25 kHz after about 3 ms.

The explanation, surely, is that the vibrating string has hit some other part of the structure. There are various possibilities, but a plausible culprit is the fret closest to the nut. The early part of the transverse string motion following the pluck is quite close to the familiar pattern for an ideal textbook string: after half a cycle, the string shape becomes an approximate mirror image of the initial displacement. The maximum displacement thus occurs 30 mm from the nut, fairly close to the first fret at about 37 mm. If the string hits a metal fret, a short force pulse is likely to occur. This would excite additional vibration, with a different pattern of minima in the frequency domain because of the different excitation pattern.

Furthermore, if the original pluck was band-limited as in the case of the thumb plucks shown in Figure 1, a fret impact could excite vibration over a far wider bandwidth, just as was seen in the measurements.

A feature of the measured response for string 1 in Figure 13 is consistent with this idea. Careful inspection shows that the brightest stripes around 3 and 6 ms appear to be more or less horizontal: they do not show the curvature associated with wave dispersion in the stiff string. But the values of bending stiffness and the predictions of the linearised theory have been verified earlier (see Figure 4), so there should not be much doubt about the value of the group velocity for transverse vibration of this string. However, if the strong signals at high frequency are caused by impacts, the timing should reflect the fact that the relevant string disturbance travelled to the impact point at a group velocity relevant to a lower frequency, and then some of its energy was scattered to high frequencies so that it would travel back to the measurement point at a higher speed. The result is that the ridge might be delayed, and also that multiple ridges might be created by different scattering histories: at any given frequency some disturbances from the initial pluck will still be travelling at the linearised group velocity, together with additional disturbances created by each impact — there might be more than one. That is roughly what the plot shows: a complicated mixture of ridges with different arrival times.

To dig deeper into the details would require explicit modelling of the impact process, and this is not attempted here. It should be emphasised that the main hypothesis put forward here is that nonlinear interactions between the vibrating string and other parts of the structure form a major ingredient of the observed behaviour. The suggestion that this interaction takes the form of one or more impacts with the first fret is simply an indication of one possibility: in the actual experiment other frets might be involved, as might some kind of interaction with the detailed end conditions as the string passes into the locating groove in the nut, or as it passes over the bridge saddle.

The original observation, that lighter-gauge strings sound brighter, would on this hypothesis be explained by the simple fact that a player will naturally tend to excite a lower-tension string to larger amplitude, and thus make impacts or other nonlinear interactions more likely. In the case of wire plucks, the pluck force is explicitly kept constant, so that different amplitudes of string motion are excited as shown in Figure 6. Musicians will probably not be thinking about plucking force as such, but they will be aware of the loudness of sound they wish to create. To achieve comparable loudness on strings of different tensions will require a larger vibration amplitude in a lighter string.

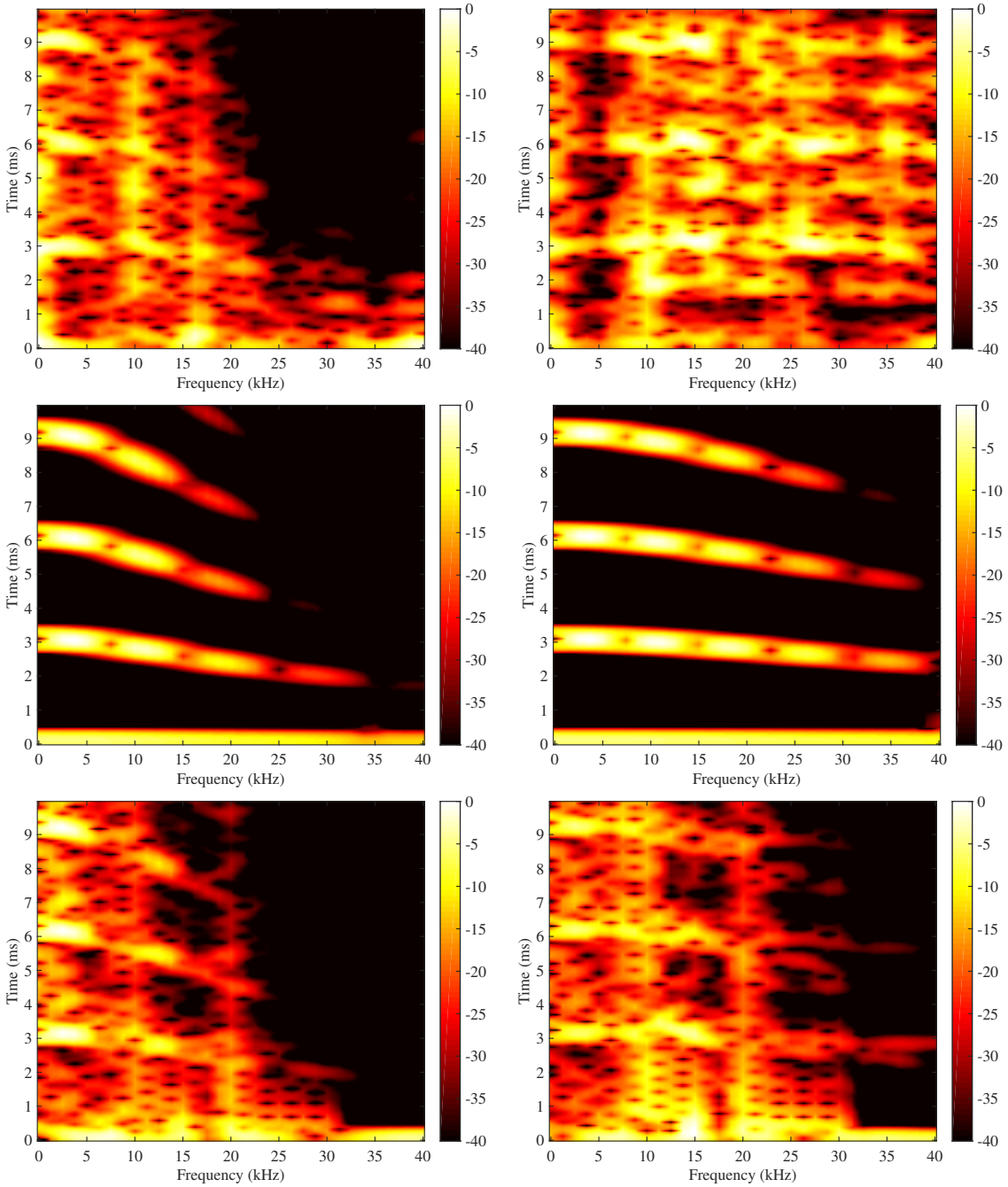

Figure 13: Spectrograms for string 4 (left column) and string 1 (right column), in a similar format to Figure 10 but calculated with shorter individual FFTs to discriminate early-time behaviour. Top row: wire-pluck measurements; middle row: linear synthesis; bottom row: combined linear/nonlinear synthesis. (Colour online.)

6 Summary and conclusions

Measurements have been discussed of the vibration of plucked strings of different gauges, in an effort to explain the observation that the sounds created by these strings are very different. Four monofilament nylon strings were considered, all fitted to a single guitar, with the same length and tuned to the same fundamental frequency. The diameters of the strings ranged over about a factor of 2, resulting in tensions varying by a factor of 4, and other physical properties varying as shown in Table 1. For the purpose of clear comparisons with theoretical modelling the strings were plucked using the wire-break method, which gives a step input of force at a single point on the string, with reliable amplitude and good control over the position and orientation.

As a first step, the measurements were analysed to calibrate the parameters of a linear model, including the effects of bending stiffness and frequency-dependent damping. If these two effects are omitted from consideration, as in the familiar idealised model used in elementary accounts of the motion of a plucked string, the string radius a plays no role whatever in the string response to an idealised wire pluck. Adding the two effects back in, very satisfactory agreement was shown between theory and measurements, leading to subtle but clear influences of a on the predicted behaviour. However, synthesis of the pluck response based on this calibrated and verified linear model failed to reproduce all the effects seen in the measurements. Furthermore, informal listening tests using the resulting sound files revealed that the differences in sound, although perceptible, were very subtle.

In the course of testing the linear model, evidence was shown of a nonlinear effect of a predominantly quadratic nature. This is probably associated with coupling between transverse and axial motion of the string. To obtain a first estimate of what this interaction might produce, a leading-order calculation has been presented in which the transverse string motion was assumed to follow the linear prediction, and then the axial motion driven by this assumed transverse motion was computed. This calculation gave a good match to the observed set of frequency-doubled components in the frequency spectra of the plucked strings. Some observed features of the transient response were also matched, at least qualitatively: in particular, clear evidence was seen in both measurements and simulations of certain of the axial resonances of the strings. However, some features were not reproduced, and again informal listening tests revealed that the audible effect of this coupling to axial string motion was quite subtle.

Another nonlinear effect was needed to explain the observations, both in terms of measurements and of perceived sound. Based on the evidence presented here, it has been suggested that the key mechanism is some kind of contact between the vibrating string and other parts of the structure of the instrument, such as the frets. A musician or instrument maker would probably call this a "buzz", but that term is usually applied to cases of multiple impacts with a fret so that a sustained effect is clearly audible. Guitar makers normally go to some lengths to avoid such buzzes. It is suggested here that, by contrast, a similar effect at a low level is probably *essential* to the tone quality of the lute, and other early plucked-string instruments in which the flesh of the fingers is used, rather than fingernails or any kind of plectrum. If a modern guitar is played in the style of a lutenist, the sound is muffled and unsatisfactory. The brightness and crispness of tone associated with the lute and related instruments probably relies on their light-gauge stringing, via some manifestation of the effect discussed here.

Deliberate musical use of string-buzzing effects is by no means an unknown phenomenon. In medieval Europe, at around the same time as the first flowering of the lute, the "bray harp" was also in use [21]. These harps had pins deliberately fitted to make occasional buzzing contact with the vibrating strings. The result is a very distinctive sound, well-described by the name of the instrument. More familiar to a contemporary audience, perhaps, is the use of deliberate string buzzing in Indian instruments such as the sitar, tanpura and veena. Those instruments have broad, almost flat bridges, quite unlike the rather sharp bridge saddle of a modern guitar. The strings may simply lay across the gently curved surface, so that they stay very close to the bridge surface for a centimetre or two after the point of lift-off. Alternatively, in some cases pieces of thread are carefully inserted so that the strings are slightly lifted from the bridge behind the "hump" of the curve so that they approach very close to that hump. Both possibilities allow the kind of nonlinear interactions suggested here, and these account for the characteristic sound of these Indian instruments (see for example [22, 5]).

In the context of the lute, the idea put forward here has some interesting consequences. First, certain design details of the instrument are perhaps clarified. The frets on a lute (or a viol, or other stringed instruments of this early period) are typically made of lengths of gut tied around the neck of the instrument. The result is softer than a modern metal fret, and this may reduce the abruptness of a

string-fret contact so that the contact force is more band-limited and the sound is less obtrusive than a buzz on a guitar. In early lutes, the frets were conventionally tied with a doubled length of gut. This slightly curious feature is, perhaps among other things, a "buzz promoter". If the vibrating length of the string is terminated at the rear strand of the fret, then the front strand could interact with the vibration as suggested here, in a somewhat similar way to the bridge of the sitar.

Another consequence is that, as with the sitar and its relatives, the desired effect of the buzzing contact would be expected to be extremely sensitive to the set-up of the instrument. The maker is probably able to shape the sound by adjusting various small details, but it is also likely that the sound is quite sensitive to changes in temperature and humidity which may cause movement in the wood structure of the instrument body and change the set-up details. To a musician, the instrument may seem rather "twitchy" to changes in the weather.

There is another effect on the sound of a lute connected with humidity sensitivity, to do with the way the instrument is played. The recommended technique is to press down with the flesh of a finger pad on a string (or a pair of strings, since lutes are mainly strung with strings in pairs), then pull sideways. The "pluck" is thus produced by frictional slipping against the skin. It is well known that the coefficient of friction of human flesh is sensitive to the state of hydration: dry skin has lower friction [23, 24, 25]. That means that when a player has dry skin, they will have to press down harder to increase the normal force in order to achieve the required frictional force for a pluck of a given strength. This will change the orientation of the string vibration, and the extra normal displacement may make buzzing more likely. The result is that the instrument may sound harsh.

This fits well with the experience of players, who know that soaking their hands to hydrate the skin can have a big effect on tone quality. Once this mechanism is understood, it can be seen that players may have other choices to achieve the same effect: there are various substances available to enhance friction. Powdered rosin is one, but this makes the fingers feel undesirably sticky. A better option may the "chalk" (magnesium carbonate powder) that rock climbers use to improve friction in their finger-tips. The effect may be longer-lasting than that of hydration, if playing in a dry environment.

As a final comment, it may be worth exploring whether any related effects occur in fretless instruments like the violin. A stopped violin string lifts gently away from the fingerboard in a very similar way to a sitar string. Do nonlinear interactions occur, which have a measurable influence on the sound and playing behaviour of a violin string? The predominant excitation of a violin string by bowing is in the plane parallel to the fingerboard surface, so this will reduce any effect, but even so there will be some motion in the perpendicular plane and this may produce nonlinear interactions.

7 Acknowledgements

The author thanks Nicolas Lynch-Aird and several colleagues in the Cambridge University Engineering Department for helpful discussions on this work.

8 Supplementary material

Sound files of the measured and synthesised pluck responses discussing this paper may be found at **LINK**.

References

[1] C. H. Hodges, J. Power, and J. Woodhouse, "The use of the sonogram in structural acoustics and an application to the vibrations of cylindrical-shells," *Journal of Sound and Vibration*, vol. 101, no. 2, pp. 203–218, 1985.

[2] J. W. S. Rayleigh, *The theory of sound*. London,: Macmillan and co., 1877.

[3] A. Chaigne, "Viscoelastic properties of nylon guitar strings," *Catgut Acoustical Society Journal*, vol. 1, no. 7, pp. 21–27, 1991.

[4] N. Lynch-Aird and J. Woodhouse, "Mechanical properties of nylon harp strings," *Materials*, vol. 10, p. 497, 2017.

[5] C. Valette, *The mechanics of vibrating strings*, pp. 116–183. New York: Springer-Verlag, 1995.

[6] J. Woodhouse, "Plucked guitar transients: Comparison of measurements and synthesis," *Acta Acustica United with Acustica*, vol. 90, no. 5, pp. 945–965, 2004.

[7] J. Woodhouse, "On the synthesis of guitar plucks," *Acta Acustica United with Acustica*, vol. 90, no. 5, pp. 928–944, 2004.

[8] R. H. Lyon and R. G. DeJong, *Theory and application of statistical energy analysis*. Boston: Butterworth-Heinemann, 2nd ed., 1995.

[9] J. Woodhouse and R. S. Langley, "Interpreting the input admittance of violins and guitars," *Acta Acustica United with Acustica*, vol. 98, no. 4, pp. 611–628, 2012.

[10] E. Skudrzyk, "The mean-value method of predicting the dynamic-response of complex vibrators," *Journal of the Acoustical Society of America*, vol. 67, no. 4, pp. 1105–1135, 1980.

[11] J. Woodhouse, "On the playability of violins: 1. reflection functions," *Acustica*, vol. 78, no. 3, pp. 125–136, 1993.

[12] N. H. Fletcher and T. D. Rossing, *The physics of musical instruments*. New York: Springer, 2nd ed., 1998.

[13] M. E. Mcintyre and J. Woodhouse, "Influence of geometry on linear damping," *Acustica*, vol. 39, no. 4, pp. 209–224, 1978.

[14] C. H. Hodges and J. Woodhouse, "Theories of noise and vibration transmission in complex structures," *Reports on Progress in Physics*, vol. 49, no. 2, pp. 107–170, 1986.

[15] H. A. Conklin, "Generation of partials due to nonlinear mixing in a stringed instrument," *The Journal of the Acoustical Society of America*, vol. 105, pp. 536–545, 1999.

[16] R. J. Hanson, J. M. Anderson, and H. K. Macomber, "Measurements of nonlinear effects in a driven vibrating-wire," *Journal of the Acoustical Society of America*, vol. 96, no. 3, pp. 1549–1556, 1994.

[17] C. Gough, "The nonlinear free-vibration of a damped elastic string," *Journal of the Acoustical Society of America*, vol. 75, no. 6, pp. 1770–1776, 1984.

[18] B. Bank and L. Sujbert, "Generation of longitudinal vibrations in piano strings: From physics to sound synthesis," *The Journal of the Acoustical Society of America*, vol. 117, no. 4, pp. 2268–2278, 2005.

[19] P. M. Morse and K. U. Ingard, *Theoretical acoustics*. Princeton, N.J.: Princeton University Press, 1986.

[20] H. A. Conklin, "Design and tone in the mechanoacoustic piano: Part III piano strings and scale design," *The Journal of the Acoustical Society of America*, vol. 100, pp. 1286–1298, 1996.

[21] S. R. Cook, "The presence and use of brays on the gut-strung harp through the 17th century," *Historical Harp Society Bulletin*, vol. 8, no. 4, pp. 2–39, 1998.

[22] A. J. M. Houtsma and E. M. Burns, "Temporal and spectral characteristics of tambura tones," *The Journal of the Acoustical Society of America*, vol. 71, no. S1, pp. S83–S83, 1982.

[23] S. Comaish and E. Bottoms, "The skin and friction: Deviations from amonton's laws, and the effects of hydration and lubrication," *British Journal of Dermatology*, vol. 84, no. 1, pp. 37–43, 1971.

[24] A. Cua, k. P. Wileherim, and H. I. Maiback, "Frictional properties of human skin: relation to age, sex, and anatomical region, stratum corneum hydration and transepidermal water loss," *British Journal of Dermatology*, vol. 123, pp. 473–479, 1990.

[25] M. Lodén, H. Olsson, T. Axéll, and Y. W. Linde, "Friction, capacitance and transepidermal water loss (tewl) in dry atopic and normal skin," *British Journal of Dermatology*, vol. 126, no. 2, pp. 137–141, 1992.